A CASE OF LEFT-HAND SPLITING OF SUPERCELL CONVECTIVE STORM AND THREE-DIMENSIONAL NUMERICAL SIMULATION

Z.Dimitrovski[1] V.Spiridonov[1],

[1]Hydrometeorological Institute, Skopje, Macedonia

Abstract

The structure and evolution of the super cell storm, observed over northern eastern part of Macedonia on 9 July 2008, is described through a combined observational radar analysis and numerical modeling study. This convective cloud system was long-lived and exhibited characteristics similar to those of classic super cells, including a cell splitting. The development and evolution of the super cell storm was simulated using a cloud resolving model with upgrade version of bulk- parameterization microphysics scheme. This was a very specific situation to simulate. The main characteristics of convective storm, structural and evolutionary properties are examined by analysis of the basic dynamical, microphysical and radar reflectivity parameters. The storm structure and evolutionary properties are evaluated by comparing the modeled radar reflectivity to the observed radar reflectivity. A three dimensional simulation using higher grid resolution mode exhibits interesting features which include a double vortex circulation, cell splitting and, secondary cell formation. The objective of this paper is to promote radar observation for evaluation of numerical cloud model prediction of severity of possible Cb development.

The convection was initiated with a warm bubble (1.3 °C perturbation) oriented in a WSW to ENE line according to the main convective mass movement. Using the same initiation protocol in each of the numerical experiments will produce a slightly different storm structures and evolution because of the different spatial and temporal resolutions employed in each model. Showing how each model run responds to the same initiation is valuable in itself. Simulations were integrated for a 1.5 hour period. A super cell convective storm is simulated by using a cloud-resolving model. Numerical experiments have been performed in 3-d by using the same domain size, with a different spatial and temporal resolution of the model. High resolution cloud model has been shown to represent convective processing quite well. Running the model in a high resolution mode, gives a more realistic view of the life cycle of convective storm, internal structure and storm behavior. The storm structure and evolutionary properties are evaluated by comparing the modeled radar reflectivity to the observed radar reflectivity. The comparative analysis between physical parameters shows good agreement among both model runs and compare well with observations, especially using a fine spatial resolution. The lack of measurements of these species in the convective outflow region does not allow us to evaluate the model results with observations. A three dimensional simulation using higher grid resolution mode exhibits interesting features which include a double vortex circulation, cell splitting and, secondary cell formation.

Keywords: Convective storm, Numerical experiment, dynamics, microphysics, reflectivity, radar observations.

1. INTRODUCTION

Convective clouds and storms represent one of the most important and challenging problems for forecasters. The severe local storms and deep convective clouds are characterized by the enhanced transport of heat and moisture in the upper layers, very strong self-organized flow fields, a very complex microphysical transformations and stratospheric penetrations, rapid evolution and dissipation processes. The precipitation processes are activated in very limited time interval and space and their intensities are manifested by large natural variability. Supercell storms are perhaps the most violent of all storm types, and are capable of producing damaging winds, large hail, and weak-to-violent tornadoes. They are most common during the spring across the mid-latitudes when moderate-to-strong atmospheric wind fields, vertical wind shear and instability are present. The degree and vertical distribution of moisture, instability, lift, and especially wind shear have a profound influence on convective storm type. It is generally recognized that the environmental buoyancy and vertical wind shear have important effect on the characteristics of convective storms.

Convective-scale model or cloud resolving model can be used to obtain general characteristics of these sub-grid processes like storm structure, upward transport of air and movement, radar reflectivity, wind speed and direction, outflow heights.

The main objective of numerical experiments performed here is to simulate the supercell storm structural and evolutionary properties by using different model initializations in respect to spatial and temporal resolution. Model is initialized on upper air sounding representing initial vertical profile of meteorological data. Three-dimensional (3-D) numerical experiments have been carefully setup in order to simulate storm dynamics, microphysics and rainfall processes. The storm structure is evaluated by comparing the modeled and simulated radar reflectivity through examination of its horizontal and vertical cross sections. In Section 2, we briefly describe the convective cloud model, numerical technique and boundary conditions. Numerical experiment and the initial conditions and the experimental setup are representing in Section 3. Then we focus on the results of sensitivity experiments with constructive discussion about the thermodynamic conditions, physical properties of clouds as well as radar reflectivity comparison. Then modeled physical data are compared with observations. Finally, results are discussed and summarized in the last section.

2. THE MODEL

2.1. Model Characteristics

The convective cloud model is a three-dimensional, non-hydrostatic, time-dependant, compressible system using the dynamic scheme from Klemp and Wilhelmson (1978). The thermodynamic energy equation is based on Orville and Kopp (1977) with effects of the snow field added. Bulk water parameterization is used for simulation of microphysical processes. Six categories of water substance are included: water vapour, cloud water, cloud ice, rain, snow and graupel or hail. Cloud water and cloud ice are assumed to be monodisperse, with zero terminal velocities. Rain, hail and snow have the Marshal-Palmer type size distributions with fixed intercept parameters. Curic and Janc (1995, 1997) proposed considering the hail size spectrum which includes only hail sized particles (larger than 0.5 cm in diameter; hereafter called realistic hail spectrum). Four prognostic conservation equations for the exchanges of water substances are considered in the model. One of the prognostic variables is the sum mixing ratios for

water vapour, cloud water and cloud ice. Other prognostic variables are the mixing ratios of rain, graupel or hail and snow. It takes into account 6 water variables (water vapour, cloud droplets, ice crystals, rain, snow, and graupel).
More detailed information regarding the hydrodynamic equations, microphysics equations, turbulent closure and numerical methods could be found in Telenta and Aleksic (1988) and (Spiridonov and Curic, 2003; 2005).

2.2. Numerical techniques

Model equations are solved on a staggered grid. All velocity components u_i are defined at the edges of the grid, while scalar variables are defined at the mid point of each grid. While the size of the model domain was the same, configured to a 61 x 61 x 16 km^3, the resolution of the model was different. The first numerical experiment is performed with resolution 1km x 1km x 0.5km with a temporal resolution of 10 s for large time. The second run of the model was set up at a very high horizontal resolution of 0.5x0.5x 0.25km^3, using a smaller time step of Δt=5s. Time splitting procedure is applied in both model runs by using a smaller time step of 2s. for solving a sound waves. At the top of the model a rigid lid (w=0) is used; a damping layer at the top of the domain was not included.

3. Model results

3.1 Description of the case

The structure and evolution of the supercell storm, observed over northern eastern part of Macedonia on 9 July 2008, is described through a combined observational radar analysis and numerical modeling study. This convective cloud system was long-lived and exhibited characteristics similar to those of classic supercells, including a cell splitting. The development and evolution of the supercell storm was simulated using a cloud resolving model with upgrade version of bulk- parameterization microphysics scheme. The convection was initiated with a warm bubble (1.3 °C perturbation) oriented in a WSW to ENE line according to the main convective mass movement. Using the same initiation protocol in each of the numerical experiments will produce a slightly different storm structures and evolution because of the different spatial and temporal resolutions employed in each model. Showing how each model run responds to the same initiation is valuable in itself. Simulations were integrated for a 1.5 hour period. This was a very specific situation to simulate. The main characteristics of convective storm, structural and evolutionary properties are examined by analysis of the basic dynamical, microphysical and radar reflectivity parameters.

3.2. A three-dimensional simulation of supercell storm

A three-dimensional simulations of August 9, 2009 supercell storm case indicates that the results are sensitive to the initial conditions. Fig. 2 shows three-dimensional views of the supercell storm life cycle at 15, 30, 45, 60, 75 and 90 min of the simulation time using a coarser spatial resolution of 1000x1000x500m^3 and time step of Δt=10s. The general supercell storm appearance is shown through distribution of mixing ratio of cloud water, cloud ice, hail, snow and rainwater during simulation time. Initial cloud water has occurred in 15 min after the initiation. Hail is formed in 25 min while cloud ice, rainwater and snow have occurred in 30 min, respectively. The modeled cloud penetrates the stable layer

and than experiences an intensive growth, developing into vigorous supercell storm with formation of large amount of ice crystals.

Numerical simulation of supercell storm in 25, 35, 45, 60, 75 and 90 min using finer spatial grid resolution of ($500x500x250m^3$) and smaller time step of ($\Delta t=5s$) is depicted on Fig. 3. It is clearly illustrated that model run with high resolution mode show a more realistic view of the supercell storm structure and evolution. Initial cloud water in this model run has occurred 12 min after initiation. It is also evident that supercell storm exhibits cell splitting especially early in its lifetime. Even though this storm started small (left), it had no problem dividing itself in two cells, as the result surrounding winds that supported both leftward movers which tend to spin clockwise (anticyclonic) and rightward moving cell which turns counterclockwise (cyclonic). The reasons for supercell storm splitting involve concepts of fluid dynamics and treatment of sub-grid scale processes, both in the original storm and its environment.

3.3 Comparison with observations

3.3.1 Cloud top history

According to observations, best estimate of the cloud top history is that the top was about 180 mb (-59°C) at the time of the first penetration; then it rose to about 110 mb (-63.5°C) or 16 km height in its developing stage and sank gradually in mature stage. The model cloud, on the other hand consistently has a lower cloud tops. At 25 min, the time we identify as corresponding to the first penetration, cloud top was at about 218 mb (-46.3°C), rising up to the 173 mb (-56°C) or 13.1 km height a.s.l. and then gradually sinking back. Thus, the model underestimates cloud top for about 63 mb.

3.3.2 Updraft velocity

Both cases show a rapid increase in peak updraft velocity at the beginning of the simulation. The maximum updraft velocity of 27.7 m/s in the first numerical experiment is calculated in 60 min of the simulation time in cloud mature stage. Model run using finer grid resolution shows increased updraft velocity of 31.3 m/s in early stage of supercell storm evolution. The height of the peak updraft reaches 7.5 km m.s.l., which is similar but somewhat higher than observations. Model runs with finer and coarser resolutions maintain peak updrafts during the remainder of the simulation for about 15.3 m s^{-1} and 11.4 m s^{-1}, respectively.

3.3.3. Liquid water contents

Radar reflectivity information is often displayed in two dimensions, making it difficult to extract the structural characteristics of convective storms. The maximum radar reflectivity and the vertical profile of liquid water distribution in a vertical column of a convective cell are used to determine a structural and intensity classification of the cell. Data set provided for the same convective case gives the pass-average values of the liquid water contents. We have calculated average LWC values for the entire horizontal cross-sections of the cloud at different vertical levels. Timing of model calculated averaged values of liquid water contents are consistent with radar observations. Comparison between the modeled and measured LWC values in the Table 1 shows a relatively good agreement with slight underestimate in heavy precipitation period which is attributed to the fallout of the precipitation in the model. These systematic differences are more evident in numerical simulation using a coarser spatial and temporal resolution, as the result of increase modeled precipitation.

3.3.4. Radar reflectivity history

The storm structure can be evaluated by comparing the modeled radar reflectivity to the observed radar reflectivity. In order to achieve that we have compared horizontal and vertical cross-sections of radar reflectivity calculated in different simulation time, with observed parameters. The first radar reflectivity echo (15:37 local time), viewed on the 10-sm radar reflectivity maps, indicates existence of one isolated convective core with 10 km diameter, slowly moving in a west-southwest line with an anvil spreading to the east-northeast. In the next 60 min. the air mass thunderstorm is successively extended affected area and separating in two cores. The frontal core is illustrating increase radar reflectivity patterns compared to backward core. In 16:38 local time a multicellular convective system has a two separate radar patterns with a maximum reflectivity echoes, greater than 60 dBz. Modeled radar reflectivity (dBz) at z=6.0 km m.s.l. after 40 min of simulation has shown a similar pattern with a slight increase magnitude of the reflectivity compared to observations. Vertical cross-section of the simulated reflectivity clearly illustrates 2 cells witch only reaches 11.5 km, m.s.l. Observations show the reflectivity top to be 14.5 to 16.5 km, m.s.l. However, during the mature stage of the storm 2 to 4 convective cells were observed. After 1 hour of simulation, the results from the model have 2-3 convective cores oriented west-northwest-northeast which is in line with the observations. The magnitude of the reflectivity is similar with observations. Only slight difference is due to 1) treatment of graupel or hail, 2) model resolution, and 3) single-moment versus multi-moment microphysics parameterizations. The width of the anvil varies among models. The observed reflectivity has an anvil width of 32-40 km at 16:12 local time, while model results range from 12.5 km to 45 km. Seifert and Weisman (2005) noted that double-moment microphysics parameterizations tend to produce broader anvils than single-moment microphysics parameterizations. The results from our study do not distinctly show this correlation. Other factors contributing to the anvil width are the graupel or hail characteristics used (which influences the particle's fall speed), the dynamics formulation, the vertical or horizontal resolution, and the number of bubbles used to initiate the convection.

Both cases show approximately the same reflectivity magnitudes somewhat extensive (>60 dBz) in cloud developing stage and slight decrease and for about 10 to 15dBz in cloud mature stage. The maximum height of the modeled reflectivity varies among runs. The reflectivity for first model run reaches 11.5 km and 12.5 km m.s.l., respectively. Early formation of precipitation, a total accumulated amount of 51.6 mm, with relatively short (20 min) heavy precipitation period appeared during the mid-latitude simulation.

4. CONCLUSIONS

Three-dimensional numerical simulations have been performed, running model using a two different initializations. First numerical experiment, is set up with resolution (1000x1000x500) m^3, with time step Δt=10 s. The second run is with spatial grid resolution of (500x500x250) m^3 and temporal resolution of 5 s. An attempt has been made to simulate a convective storm occurred on August 9, 2008 over Macedonia. Numerical simulations of the cloud system duplicate the general observational features, including horizontal and vertical dimensions, cyclic behavior and convective core and anvil characteristics. Comparison of the horizontal and vertical cross sections of radar reflectivity echoes in different time of multicell storm evolution agrees well with observations.

The intercomparison shows differences in rainfall efficiency attributed to differences in the interaction of

cloud dynamics and microphysics and precipitation flux processes. Both model runs have reproduced the observed convection with radar reflectivity reaching > 50 dBZ. Both numerical experiments simulated the development of supercell storm structure. However model run with finer grid resolutions has been more accurate in simulation of storm splitting. A three dimensional simulation using higher grid resolution mode exhibits interesting features which include a double vortex circulation, cell splitting and, secondary cell formation. We found, through the study of a model-predicted real convective system, that a very small change in the grid resolution of the model can produce very different behaviours of storms after their splitting.

Acknowledgements
Authors would like kindly to acknowledge to Macedonian State Meteorological Service for provision of initial data, radar images and rainfall data for convective case experiment.

REFERENCES

Cotton, W.R., and G. J.Tripoli (1979), Cumulus convection in shear flow 3-D numerical experiments, *J. Atmos.Sci.*, 35, 1503-1521.

Clark, T.L. (1979), Numerical simulations with a three-dimensional cloud model: Lateral boundary condition experiments and multicellular severe storm simulations, *J. Atmos. Sci.* 36, 2191–2215.

Curic, M. and D. Janc (1995), On the sensitivity of the continuous accretion rate equation used in bulk-water parameterization schemes, *Atmos. Res*., 39, 313- 332.

Curic, M. and D. Janc (1997), On the sensitivity of hail accretion rates in numerical modeling, *Tellus*, 49A, 100-107. Curic, M. ,Janc, D., and V. Vuckovic (2007), Numerical simulation of Cb cloud vorticity, *Atmos. Res*., 83, 427-434.

Durran, D. R. (1981), The effects of moisture on mountain lee waves, Ph.D. Thesis, Massachusetts Institute of Technology Boston, MA (NTIS PB 82126621).

Hsie, E.-Y., R.D. Farley and R.D. Orville, 1980: Numerical simulation of ice=phase convective cloud seeding. *J.Appl.Met.* **19**. 950-977.

Khain, A., and B. Lynn , 2009: Simulation of a supercell storm in clean and dirty atmosphere using weather research and forecast model with spectral bin microphysics, *J. Geophys. Res.*, 114, D19209, doi:10.1029/2009JD011827

Klemp, J. B. and R.B. Wilhelmson (1978), The simulation of three-dimensional convective storm dynamics, *J. Atmos. Sci.* 35, 1070-1096.

TABLE CAPTIONS

Table 1. Comparison between modelled and observed parameters. Columns shown from left to right illustrate local time of radar observation, consistent model simulation time, liquid water content, updraft speed, cloud top, radar reflectivity and rainfall intensity averaged over simulation time

FIGURE CAPTIONS

Figure 1. Upper air sounding for Skopje, Macedonia on 09 August, 2008 12 UTC taken from

Figure 2. A three-dimensional depictions of convective storm life cycle, expressed through their mixing ratios in (g kg^{-1}), viewed from the southeast (SE), at 15min time intervals starting at 15min. Plots with a corresponding yellow, blue, green, and red color denote the total condensate mixing ratios of cloud water, rainwater, snow and hail, respectively. The model was run with a spatial resolution of (1000x1000x500)m^3 and temporal resolution of 10s.

Figure 3. Same as Figure 2 except the model was set up with a finer spatial resolution of (500x500x250) m^3 and temporal resolution of 5 s.

Figure 4. Radar reflectivity (dBZ) along the SW-NE vertical cross-section. Observations from WSR-74 S/X radar upgraded with ASU-MRL at different observational time, starting at 15:37 local time.

Figure 5. Radar reflectivity (dBz) along the SW-NE vertical cross-section. Model results at 25, 35, 50, 60 and 70 min of the simulation time. Model run I.

Figure 6. Same as Figure 5, except for using a finer spatial and temporal resolution into the model initialisation. Model run II.

Figure 7. Radar reflectivity (dBZ) at z = 6.5 km m.s.l. Observations provided from WSR-74 S/X radar upgraded with ASU-MRL, in different time intervals, started at 15:37 local time.

Figure 8. Horozontal cross-section of radar reflectivity (dBz) at z=6.5 km m.s.l. Model results at 20, 35, 50. 60, 70 and 80 min of the simulation time. Model run I.

Figure 9. Same as Figure 9, ecept for using a finer resolution of the model. Model run II.

Table 1. Comparison between modelled and observed parameters. Columns shown from left to right illustrate local time of radar observation, consistent model simulation time, liquid water content, updraft speed, cloud top, radar reflectivity and rainfall intensity averaged over simulation time

Local time of radar observation	**Model time (min)**	**q (kg/m^3)**			**W (m/s)**			**Htop (km)**			**Zmax (dBz)**			**Rainfall intensity (mm/min)**		
		Model run		**Obs.**	Model run		**Obs.**	Model run		**Obs.**	Model run		**Obs.**	Model run		**Obs.**
		I	II		I	II		I	II		I	II		I	II	
15:37	20	0.8	0.9	**1.8**	15.0	16.5		9.3	11.1	**16.5**	50.2	39.5	**43.0**	0.00	0.02	**0.01**
15:53	35	4.7	5.2	**4.7**	23.8	31.1		15.3	12.4	**16.5**	70.9	61.0	**54.0**	0.01	0.81	**0.83**
16:12	50	6.6	7.3	**8.5**	24.7	31.3		15.3	13.4	**16.5**	68.4	59.0	**55.0**	0.66	0.90	**1.00**
16:24	60	9.8	10.4	**13.1**	27.3	28.2		15.8	12.7	**16.0**	66.5	50.0	**60.0**	0.92	0.75	**1.33**
16:36	70	5.4	5.7	**6.1**	17.3	16.4		15.8	12.4	**15.1**	62.8	53.0	**53.0**	0.91	0.64	**1.16**
16:48	80	3.9	4.3	**5.7**	11.4	11.3		15.8	11.1	**15.5**	57.8	37.0	**57.0**	0.85	0.56	**0.33**

Figure 1. **Upper air sounding for Skopje, Macedonia on 09 August, 2008 12 UTC taken from**

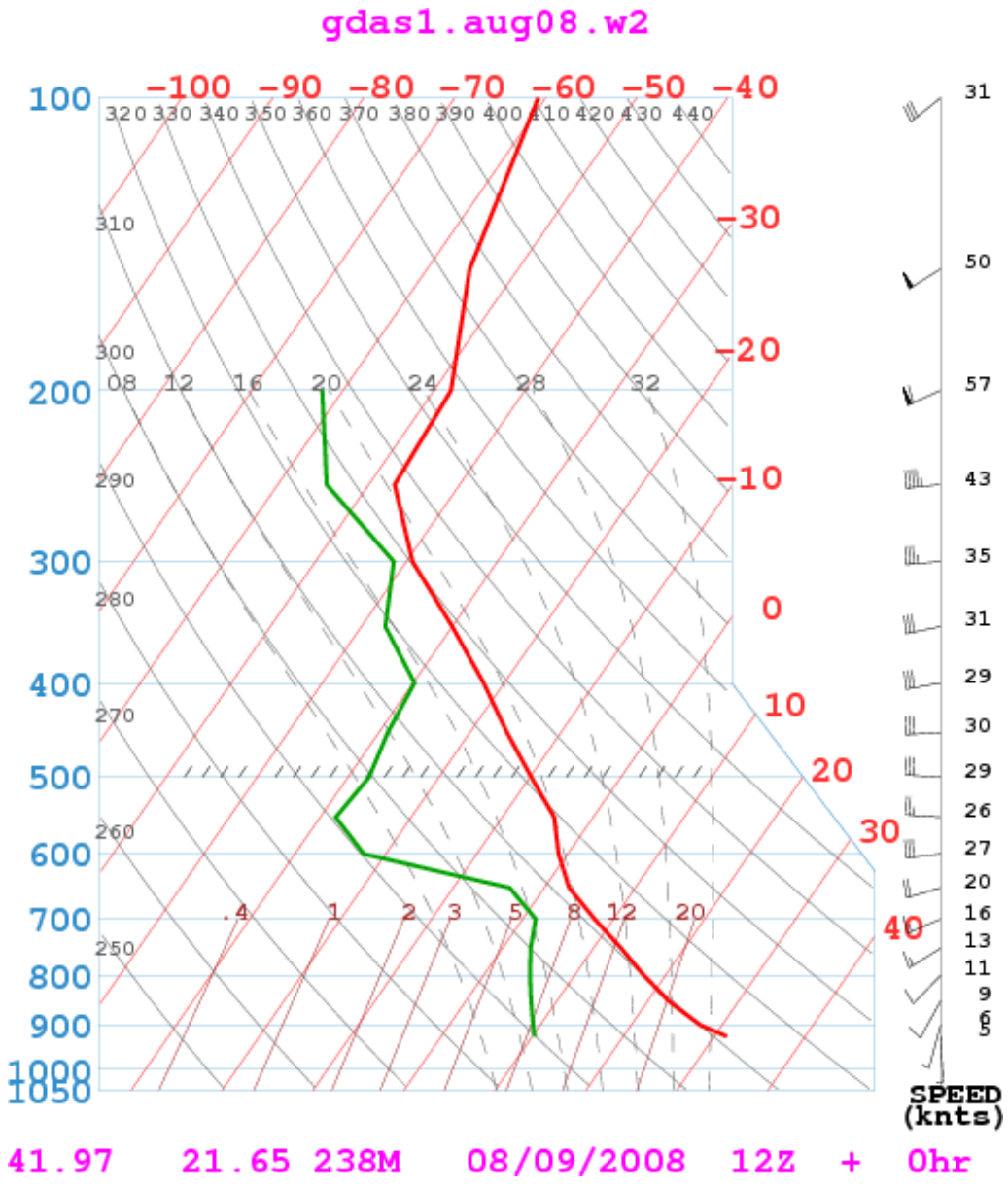

Figure 2

Figure 2. A three-dimensional depictions of convective storm life cycle, expressed through their mixing ratios in (g kg^{-1}), viewed from the southeast (SE), at 15min time intervals starting at 15min. Plots with a corresponding yellow, blue, green, and red color denote the total condensate mixing ratios of cloud water, rainwater, snow and hail, respectively. The model was run with a spatial resolution of (1000x1000x500)m^3 and temporal resolution of 10s.

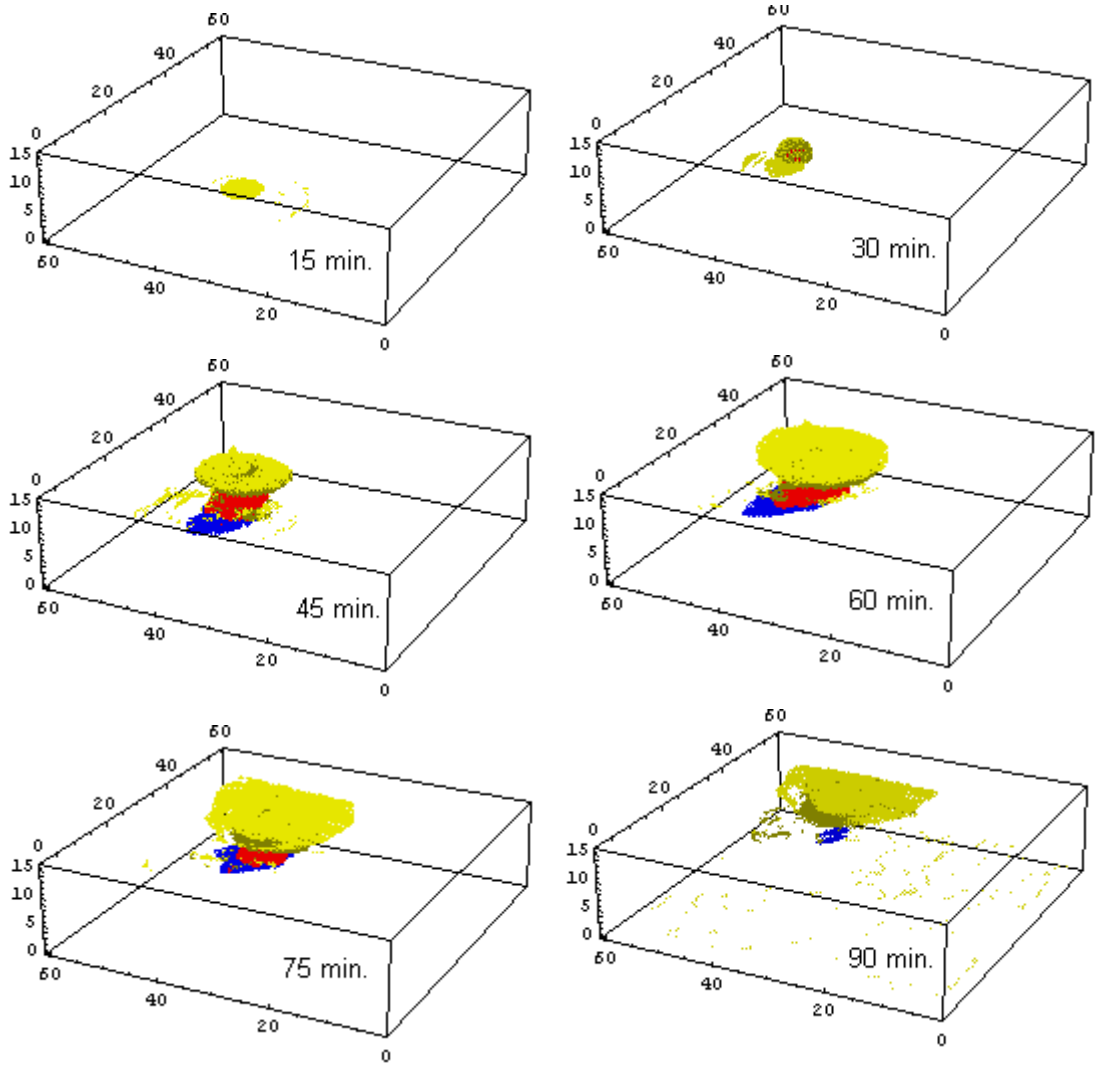

Legend:

- Cloud water +cloud ice + water vapour mixing ratio > 0.01 g/kg
- Rainwater mixing ratio > 0.01 g/kg
- Graupel or hail mixing ratio > 0.1 g/kg
- Snow mixing ratio > 0.1 g/kg

Figure 3

Figure 3. Same as Figure 2 except the model was set up with a finer spatial resolution of (500x500x250) m^3 and temporal resolution of 5 s.

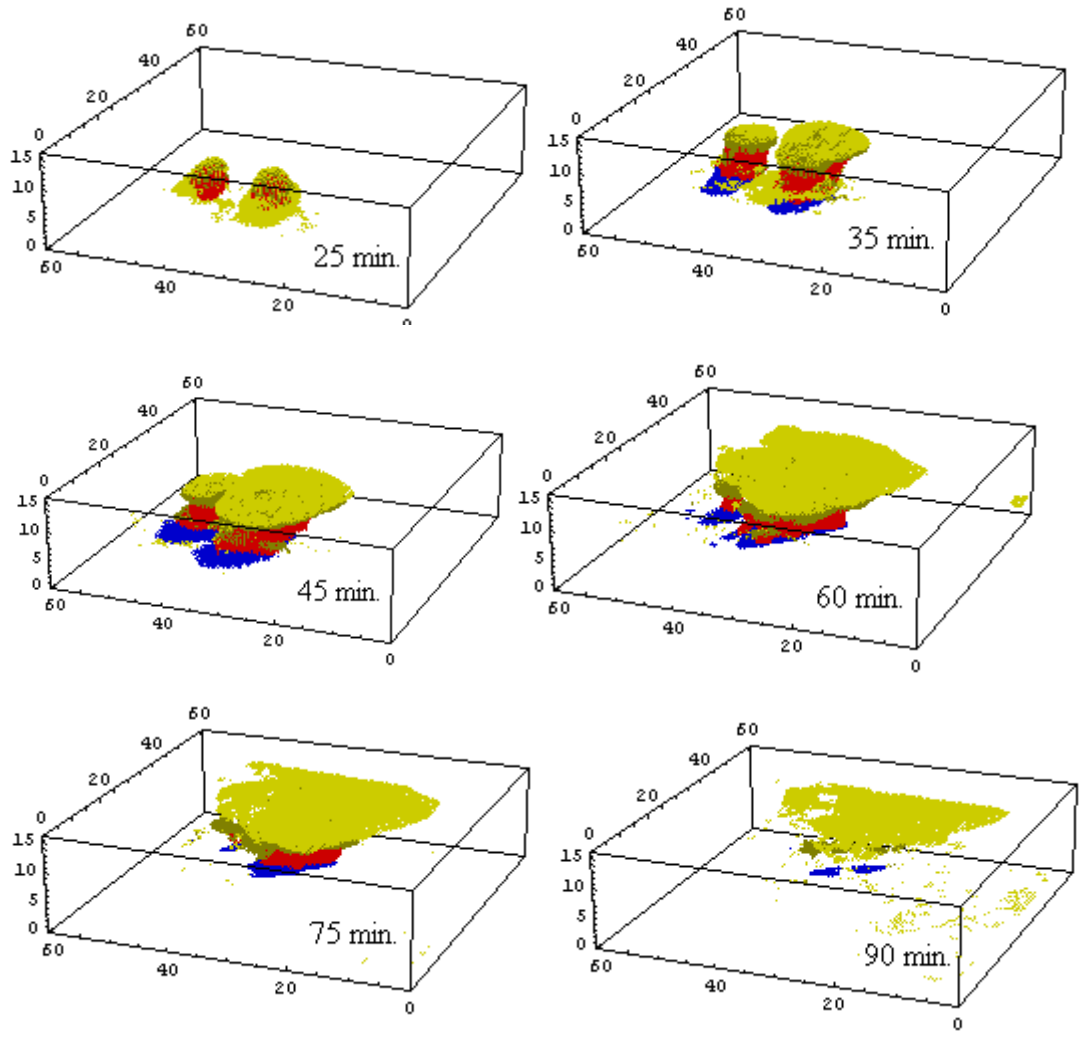

Legend:

Cloud water +cloud ice + water vapour mixing ratio > 0.01 g/kg
Rainwater mixing ratio > 0.01 g/kg
Graupel or hail mixing ratio > 0.1 g/kg
Snow mixing ratio > 0.1 g/kg

Figure 4. **Radar reflectivity (dBZ) along the SW-NE vertical cross-section. Observations from WSR-74 S/X radar upgraded with ASU-MRL at different observational time, starting at 15:37 local time.**

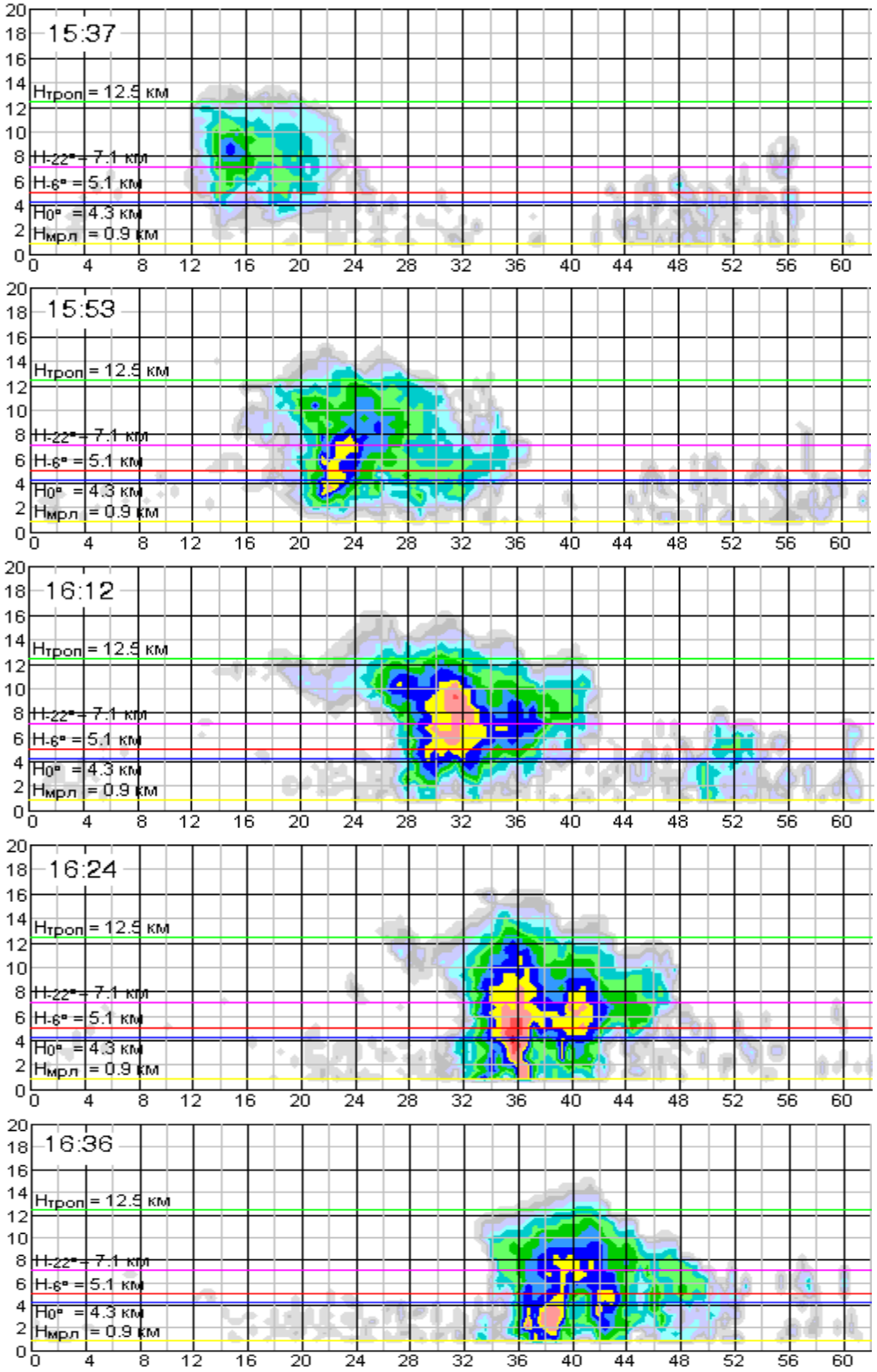

Figure 5. **Radar reflectivity (dBz) along the SW-NE vertical cross-section. Model results at 25, 35, 50, 60 and 70 min of the simulation time. Model run I.**

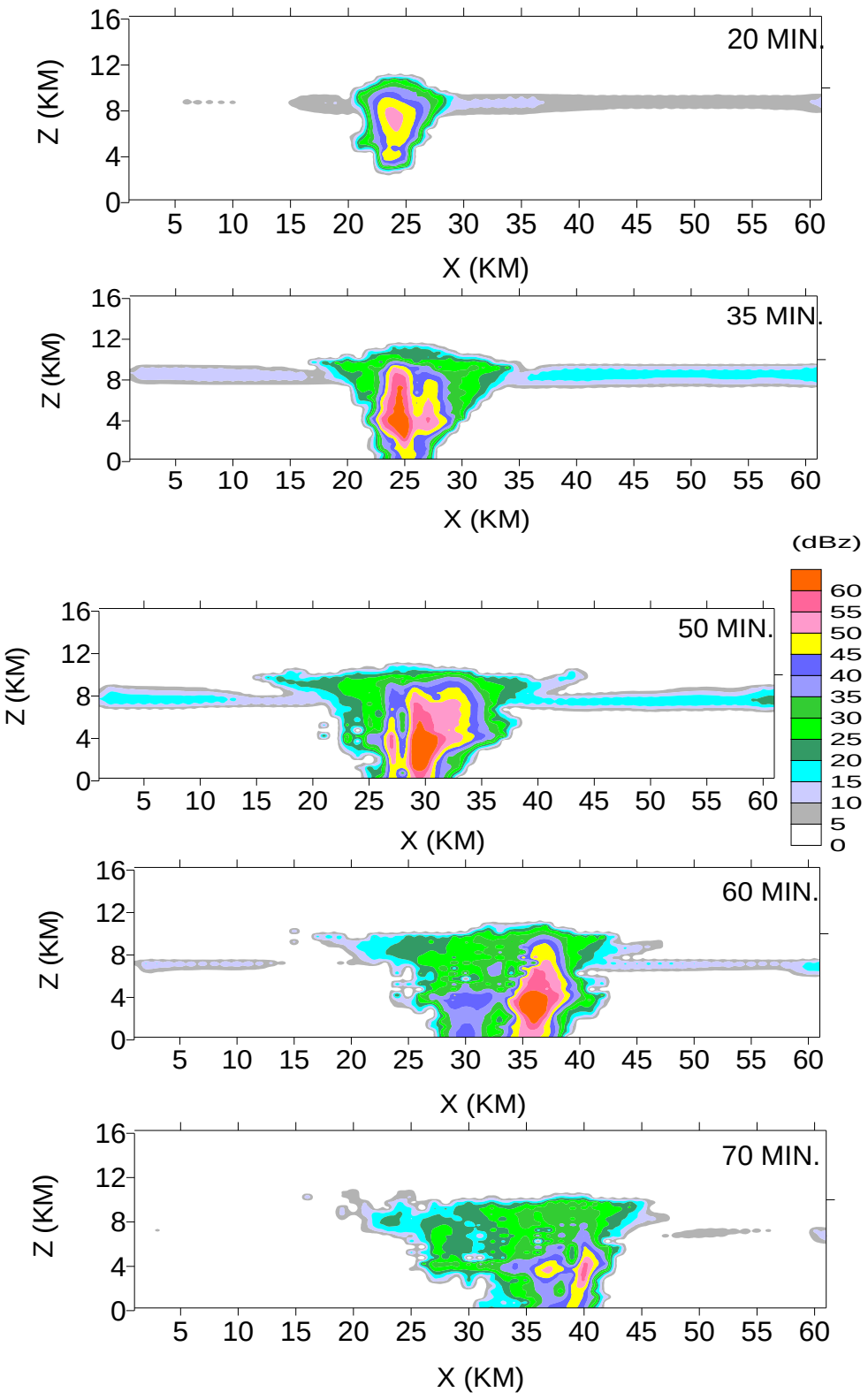

Figure 6

Figure 6. Same as Figure 5, except for using a finer spatial and temporal resolution into the model initialisation. Model run II.

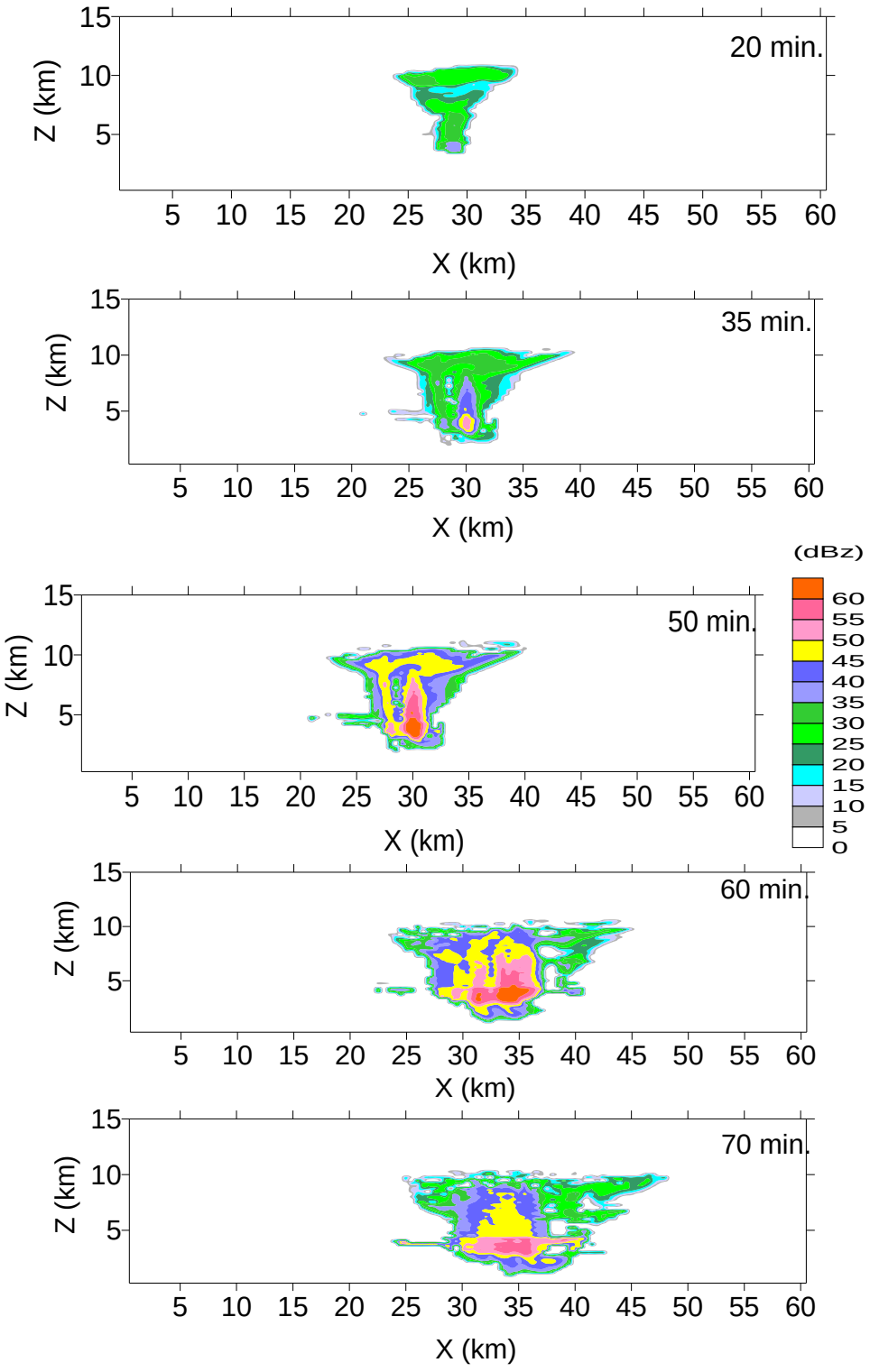

Figure 7

Figure 7. Radar reflectivity (dBZ) at z = 6.5 km m.s.l. Observations provided from WSR-74 S/X radar upgraded with ASU-MRL, in different time intervals, started at 15:37 local time.

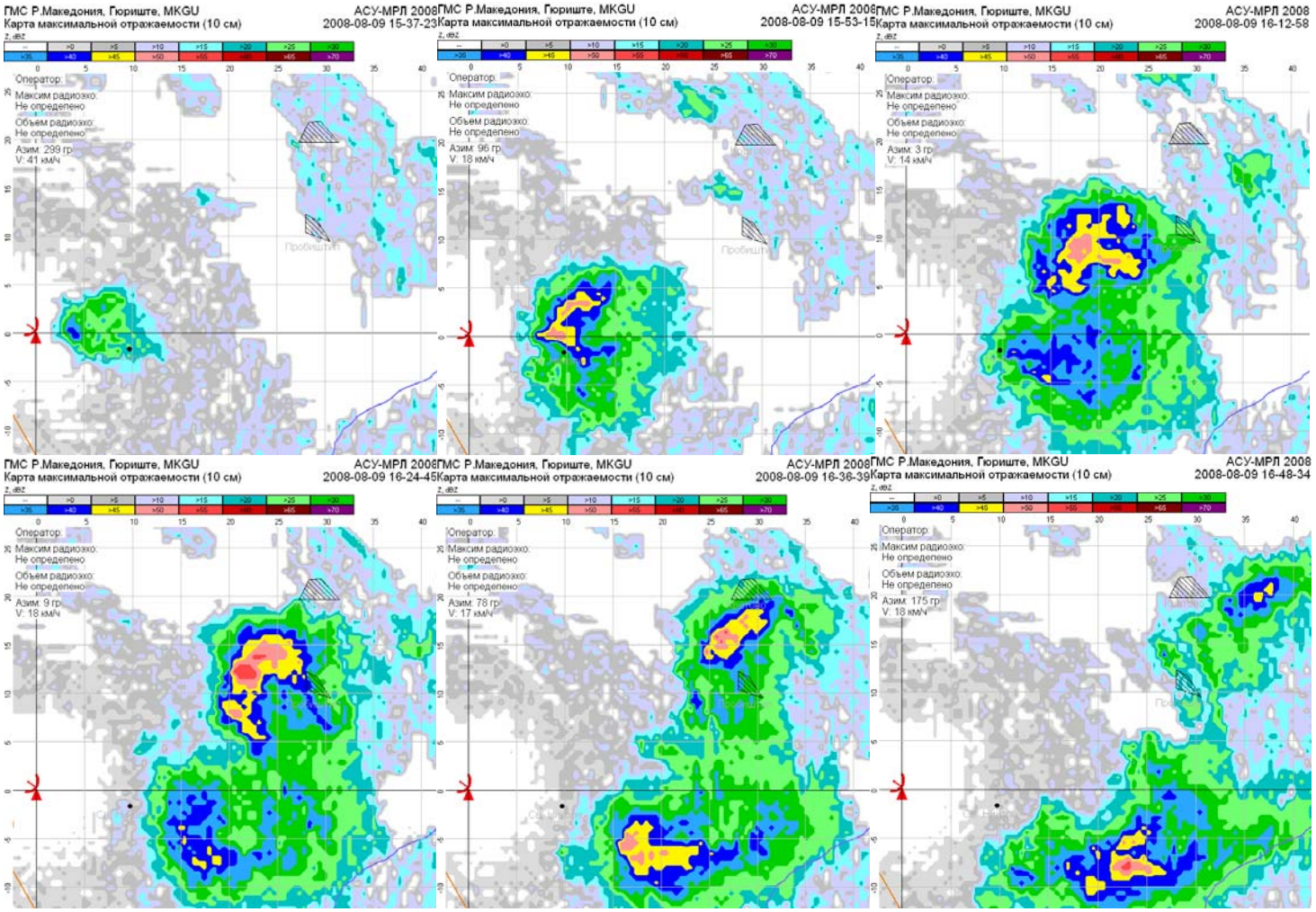

Figure 8

Figure 8. Horozontal cross-section of radar reflectivity (dBz) at z=6.5 km m.s.l. Model results at 20, 35, 50. 60, 70 and 80 min of the simulation time. Model run I.

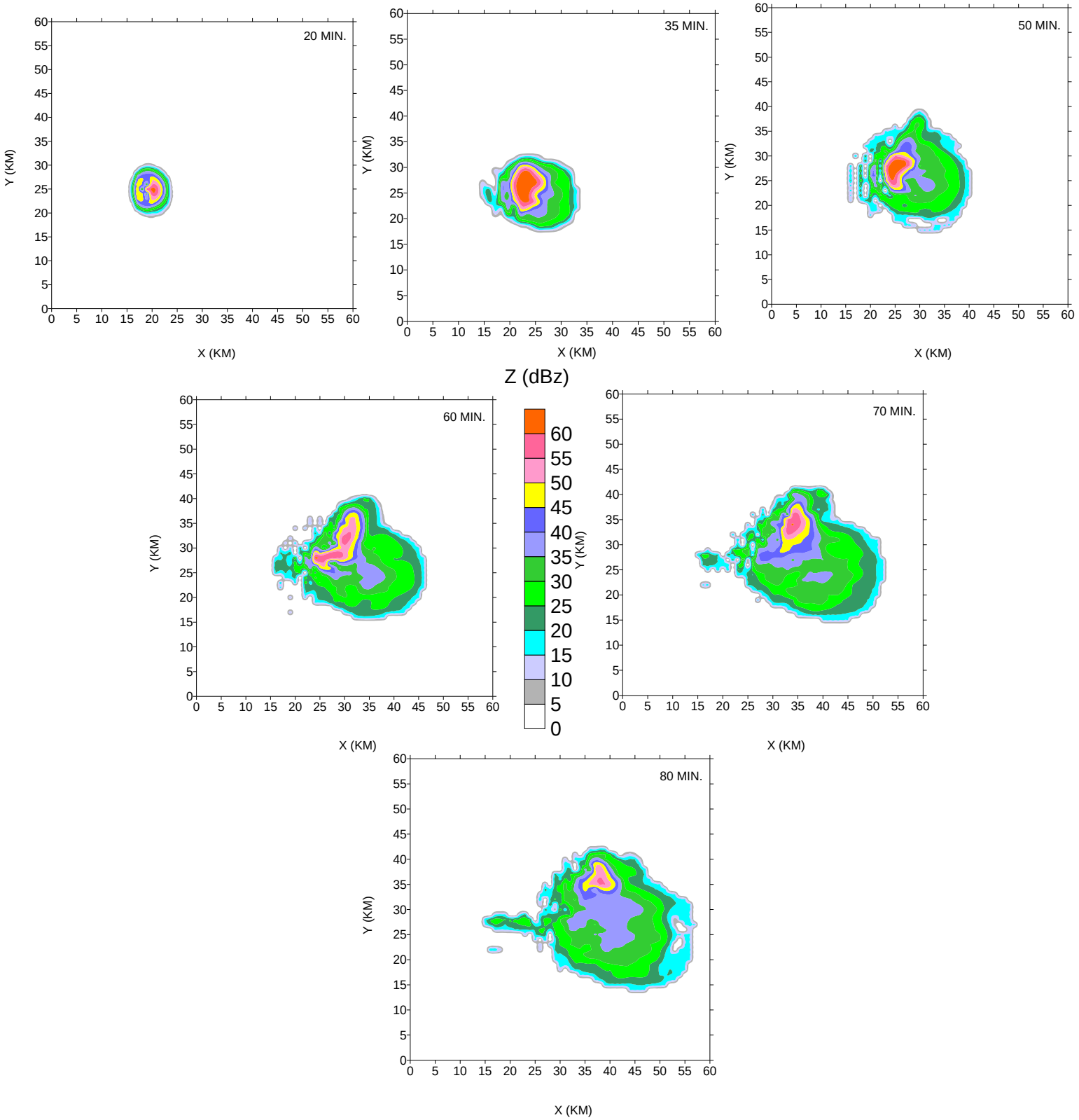

Figure 9

Figure 9. Same as Figure 9, ecept for using a finer resolution of the model. Model run II.